ence of thick clouds so that mean vertical motions should be less downward. Diabatic heating at the bottom of thick tropospheric anvils should also give rise to decreased downward motion and possibly even upward motion. At mid-tropospheric heights it is less obvious what to expect during El Niño conditions. On the one hand, the presence of thick clouds should inhibit diabatic cooling and mitigate against downward motion. On the other hand, precipitation from decaying tropospheric anvils would cause diabatic cooling due to evaporation below the clouds, leading to enhanced downward motion there.

Figure 4 shows the mean vertical motions observed at Christmas Island during the period before the 1986–1987 El Niño and during the El Niño. Upward vertical motions above 14 km were observed to be systematically lower during the El Niño, consistent with the idea of reduced diabatic heating. Downward vertical motion is reduced systematically in the upper troposphere, consistent with the idea of reduced cooling to space due to the presence of optically thick clouds; enhanced downward motions around 6 km are consistent with evaporative cooling.

Although we favor a radiative explanation for the vertical motions observed in the upper troposphere and lower stratosphere, dynamical forcing may also play a significant role. In particular, the meridional circulation needed to maintain the stratospheric quasi-biennial oscillation winds in geostrophic balance involves vertical motion near the equator (*8*), with a sign that reverses on the quasi-biennial time scale. This circulation is not expected to penetrate below the tropopause, however.

Tropical networks of wind profilers and integrated sounding systems (*9*) that include wind profilers are currently in an advanced state of development and should be implemented within the next few years. They are expected to provide observations of tropical circulation systems and equatorial waves over a broad range of scales (*10*). Furthermore, profilers by virtue of their ability to resolve small-scale internal waves provide a means for investigating dynamical coupling between the lower and middle atmosphere.

REFERENCES AND NOTES

1. B. B. Balsley, W. L. Ecklund, D. A. Carter, A. C. Riddle, K. S. Gage, *J. Atmos. Sci.* **45**, 396 (1988).
2. W. L. Ecklund, K. S. Gage, G. D. Nastrom, B. B. Balsley, *J. Clim. Appl. Meteorol.* **25**, 885 (1986); K. S. Gage, in *Radar in Meteorology*, D. Atlas, Ed. (American Meteorological Society, Boston, 1990), pp. 534–565; G. D. Nastrom, W. L. Ecklund, K. S. Gage, *Mon. Weather Rev.* **113**, 708 (1985); G. D. Nastrom, K. S. Gage, W. L. Ecklund, *Radio Sci.* **25**, 933 (1990); T. E. VanZandt, G. D. Nastrom, J. L. Green, *J. Geophys. Res.* **96**, 2845 (1991).
3. J. R. Holton, *An Introduction to Dynamic Meteorology* (Academic Press, New York, ed. 2, 1979), pp. 324–329.
4. T. G. Dopplick, *J. Atmos. Sci.* **29**, 1278 (1972); G. M. Doherty, R. E. Newell, E. F. Danielsen, *J. Geophys. Res.* **89**, 1380 (1984).
5. T. P. Ackerman, K.-N. Liou, F. P. J. Valero, L. Pfister, *J. Atmos. Sci.* **45**, 1606 (1988); P. J. Webster and G. L. Stephens, *ibid.* **37**, 1521 (1980).
6. R. E. Newell and S. J. Gould-Stewart, *ibid.* **38**, 2789 (1981).
7. A. E. Gill, *Atmosphere-Ocean Dynamics* (Academic Press, New York, 1982), pp. 472–482.
8. R. J. Reed, *Q. J. R. Meteorol. Soc.* **90**, 441 (1964); G. B. Tucker, *ibid.*, p. 405; R. A. Plumb and R. C. Bell, *ibid.* **108**, 335 (1982).
9. K. S. Gage *et al.*, *Bull. Am. Meteorol. Soc.* **69**, 1041 (1988). W. F. Dabberdt *et al.*, in *Proceedings of the Seventh AMS Symposium on Meteorological Observations and Instrumentation* (American Meteorological Society, Boston, 1991).
10. B. B. Balsley, D. A. Carter, A. C. Riddle, W. L. Ecklund, K. S. Gage, *Bull. Am. Meteorol. Soc.* **72**, 1355 (1991); K. S. Gage, B. B. Balsley, W. L. Ecklund, R. F. Woodman, S. K. Avery, *Eos* **71**, 1851 (1990); K. S. Gage *et al.*, *J. Geophys. Res.* **96**, 3209 (1991).
11. R. H. Johnson, *J. Meteorol. Soc. Jpn.* **60**, 682 (1982).
12. J. F. Gamache and R. A. Houze, Jr., *Mon. Weather Rev.* **113**, 1241 (1985).

13. The Christmas Island wind profiler is supported by the U.S. Tropical Oceans and Global Atmosphere Project Office. This research has been supported in part by the National Science Foundation under agreement ATM-8720797.

9 August 1991; accepted 16 October 1991

A Fungal Gene for Antibiotic Resistance on a Dispensable ("B") Chromosome

VIVIAN P. MIAO,* SARAH F. COVERT, HANS D. VANETTEN†

A family of cytochrome P-450 (*Pda*) genes in the pathogenic fungus *Nectria haematococca* is responsible for the detoxification of the phytoalexin pisatin, an antimicrobial compound produced by garden pea (*Pisum sativum L.*). The *Pda6* gene was mapped by electrophoretic karyotype analysis to a small meiotically unstable chromosome that is dispensable for normal growth. Such traits are typical of B chromosomes. The strains of *Nectria* studied here have no sequences that are homologous to the *Pda* family other than *Pda6* and therefore demonstrate that unique, functional genes can be found on B chromosomes. Unstable B chromosomes may be one mechanism for generating pathogenic variation in fungi.

THE ABILITY OF THE PLANT PATHOgenic fungus *Nectria haematococca* MP (mating population) VI to infect pea (*Pisum sativum L.*) is determined in part by whether the fungus can detoxify pisatin, an antibiotic produced by pea (*1*). Detoxification of pisatin is catalyzed by pisatin demethylases, a group of substrate-specific, cytochrome P-450 monooxygenases (*2*) encoded by the *Pda* gene family. Although each *Pda* gene can independently confer pisatin-demethylating ability on the fungus (a trait called Pda^+), the genes vary in their inducibility by pisatin and by the amount of resulting enzymatic activity (*3*). Only isolates of *N. haematococca* that rapidly detoxify pisatin have the potential to be aggressive pathogens on pea (*1, 4–6*).

Meiotic events in *N. haematococca* can be studied by the technique of tetrad analysis. The products of meiosis are contained in structures (asci) that allow their recovery as a set. Genetic crossing begins by the joining of a haploid cell from each parent to produce a fusion cell containing two nuclei. This cell multiplies vegetatively inside a maternally produced fruiting body (a perithecium) into a cluster of cells. Asci develop when nuclear fusion and meiosis occur within some of these cells. The four haploid products of meiosis (a tetrad) then divide mitotically, resulting in eight ascospores per ascus. Each tetrad therefore consists of four pairs of sister spores, each pair representing one of the four products of meiosis.

Some crosses of *N. haematococca* produce fewer Pda^+ progeny than expected from conventional models of inheritance (*4, 5, 7*). In a cross (cross 272) between two strains that each carried *Pda6* as the only active *Pda* gene (*7*), only asci with 8 Pda^+:0 Pda^- segregation were expected. However, many asci from this cross showed 4 Pda^+:4 Pda^- segregation (Table 1). The Pda^- condition was not associated with any distinct phenotype or growth pattern in culture. No homology to a cloned *Pda* gene (*Pda-T9*) (*8*) was detected by hybridization to the DNA from these Pda^- progeny (*9*); thus loss of

V. P. Miao, Department of Plant Pathology, Cornell University, Ithaca, NY 14853.
S. F. Covert, Department of Plant Pathology, University of Arizona, Tucson, AZ 85721.
H. D. VanEtten, Department of Plant Pathology, Cornell University, Ithaca, NY 14853, and Department of Plant Pathology, University of Arizona, Tucson, AZ 85721.

*Present address: Institute of Molecular Biology, University of Oregon, Eugene, OR 97503.
†To whom correspondence should be addressed at present address at the University of Arizona.

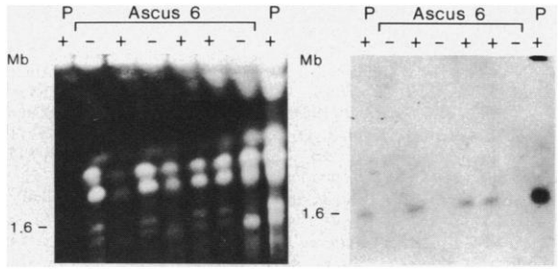

Fig. 1. Karyotypes partially resolved by pulsed-field gel electrophoresis (at left) (*9, 18*) of parent strains (P) and progeny from ascus 6 of cross 272. Plus and minus symbols indicate that a strain was Pda^+ or Pda^-, respectively. Pda^- progeny lack the 1.6-Mb chromosome, shown here at right to contain the *Pda6* locus by Southern blot hybridization to *Pda-T9* (*19*). The intensely staining bands immediately below the wells are unresolved chromosomes ≥4 Mb. Molecular sizes were estimated by coelectrophoresis of *Saccharomyces cerevisiae* strain YPH 149 (*20*) and *Neurospora crassa* strain 74-OR23-1A (*21*). In general, the second spore of a pair that represents the same meiotic product is not shown when such pairs were identified by other markers such as mating type; the six progeny portrayed represent all the products of meiosis.

the Pda^+ phenotype was due to failure to transmit *Pda6*, rather than to gene inactivation. Because asci in one perithecium are normally derived from the same initial fusion cell in fungi such as *N. haematococca*, the presence of asci with only Pda^+ progeny, as well as asci with both Pda^+ and Pda^- progeny in the same perithecium, indicates that loss of *Pda6* occurred only after crossing. Furthermore, the absence of differences between sister spore pairs representing the same meiotic product suggests that changes happened before the first division after meiosis. Therefore, failure to transmit *Pda6* could have occurred during proliferation of the fusion cell preceding meiosis, during meiosis, or both (*10*).

Pda6 mapped to a small chromosome of about 1.6 megabases (Mb) when chromosomes of the parent strains in cross 272 were resolved by pulsed-field gel electrophoresis (*11*) and probed with the cloned *Pda-T9* gene (Fig. 1). In all Pda^- progeny examined, changes involving the 1.6-Mb chromosome were apparent by electrophoretic karyotype analysis. The changes appear to be caused primarily by chromosome loss or deletion (Fig. 2). Nondisjunction was also observed; two of the Pda^+ progeny from ascus 19 (Fig. 2) have two copies of the *Pda6* chromosome, one of which is a truncated form. Most Pda^+ progeny retained the parental *Pda6* chromosome, but smaller versions of the chromosome that hybridized to *Pda-T9* were also observed (Fig. 2). To verify that the apparently lost or deleted portions of the 1.6-Mb chromosome had not translocated elsewhere in the genome, we isolated the 1.6-Mb chromosome from a pulsed-field gel and used it to probe isolates from cross 272 (Fig. 3). The 1.6-Mb chromosome hybridized to itself and its deletion derivatives of 1.5 and 0.9 Mb but not to chromosomes of the Pda^- strain that had apparently lost the chromosome.

The novel chromosomes observed in the progeny of cross 272 were themselves unstable. A Pda^+ strain with a 1.5-Mb derivative of the chromosome was crossed (cross 289) to a Pda^- sibling carrying a 1-Mb derivative chromosome from which *Pda6* was deleted (Fig. 2, ascus 6). Although the Pda phenotype of the progeny from this cross segregated as expected by Mendelian inheritance (*12*), all tetrads examined showed changes in the size of their small chromosomes. In some cases, the two parental forms of the *Pda6* chromosome appeared to have recombined between themselves to reconstruct the original 1.6-Mb *Pda6* chromosome (Fig. 4, asci 1 and 2); a presumptive reciprocal product of 0.9 Mb was also generated (Fig. 5). The preponderance of

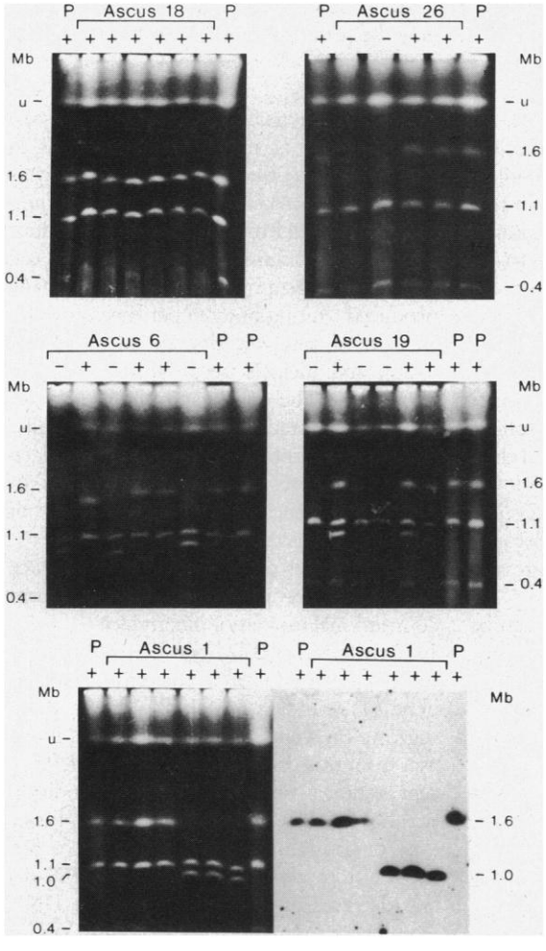

Fig. 2. Karyotypes by pulsed-field gel electrophoresis of parents and progeny from cross 272 (*22*). Progeny in ascus 18 illustrate the expected pattern. The 1.6-Mb chromosome in both parents and Pda^+ progeny of ascus 1 hybridized to *Pda-T9*, as shown in the corresponding Southern blot (at lower right). Similar results were also obtained with the parents and Pda^+ progeny of asci 6, 18, 19, and 26. Nonparental bands in Pda^+ progeny were deduced to be derivatives of the 1.6-Mb chromosome because they hybridized to *Pda-T9*. In Pda^- progeny, 0.9- to 1-Mb bands that did not hybridize to the probe also appear to be derived by deletion (Fig. 3). Unresolved large molecular-mass chromosomes are designated by u.

Table 1. Inheritance of pisatin-demethylating ability among progeny from cross 272 between two *Pda6* strains of *N. haematococca*. Asci from the same perithecium and from different perithecia were analyzed. Representatives of both segregation patterns (8 Pda^+:0 Pda^- is the expected pattern, and 4 Pda^+:4 Pda^- is the unexpected pattern) from different perithecia segregated normally for a control marker, the mating type gene *Mat*. Crossing, isolation of progeny from asci, scoring *Mat*, and assaying pisatin demethylation were as described (*4, 5*).

Perithecium	No. of asci		Progeny analyzed by pulsed-field electrophoresis
	8:0	4:4	
A	4		Ascus 1
B		9	Ascus 6
C		3	
D	2	1	Asci 18 and 19
E	1		
F	3		
G	2	1	Asci 25 and 26

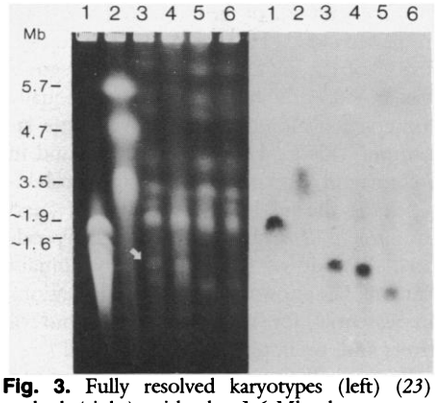

Fig. 3. Fully resolved karyotypes (left) (*23*) probed (right) with the 1.6-Mb chromosome (*24*). Lane 1, *S. cerevisiae* YPH80 (FMC BioProducts); lane 2, *Schizosaccharomyces pombe* 972 (FMC BioProducts), lane 3, Pda^+ parent from which the 1.6-Mb chromosome (arrow) was isolated; lane 4, Pda^+ progeny from ascus 6 (Fig. 2); lane 5, Pda^- progeny from ascus 6; and lane 6, Pda^- progeny from ascus 26. In all other pulsed-field gels we have run, the 1.6-Mb chromosome of *S. cerevisiae* migrated the same distance as the meiotically unstable chromosome of *N. haematococca*. As a result, we regard the migration of the *S. cerevisiae* chromosomes in this gel as an anomaly. Surprisingly, the 1.6-Mb chromosome hybridized to specific chromosomes of *S. cerevisiae* and *S. pombe* to a greater extent than it did to the *N. haematococca* strain lacking the dispensable chromosome.

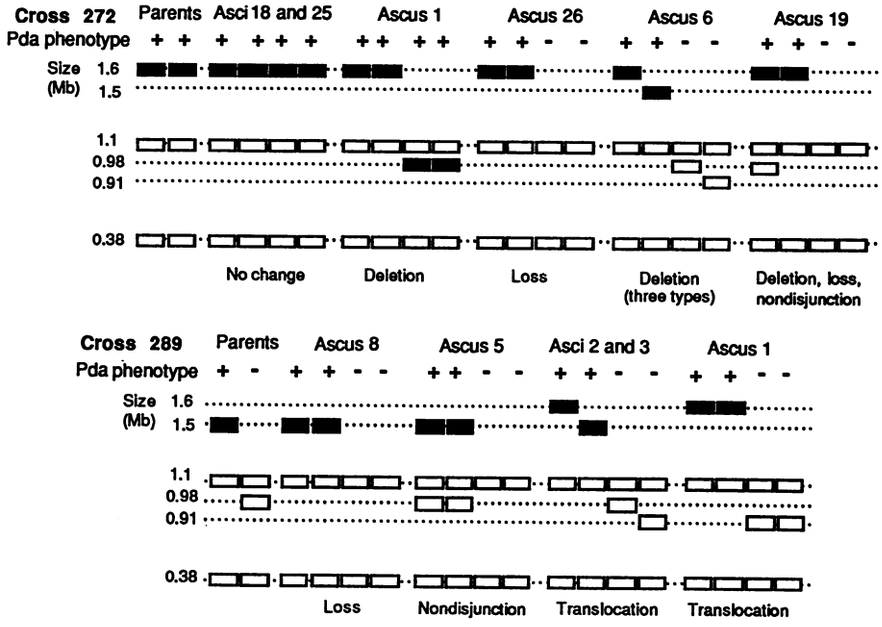

Fig. 5. Summary of partial karyotypes from parents and progeny of crosses 272 (Table 1) and 289 (*12*). The karyotypes are represented as a vertical schematic diagram of how the chromosomes would appear after separation by pulsed-field gel electrophoresis. Size (in megabases) of each chromosome is indicated to the left. Filled rectangles indicate chromosomes that hybridized with *Pda-T9*; open rectangles indicate chromosomes that failed to hybridize. Below the karyotypes are suggested cytological events that could lead to the observed patterns among the four products of meiosis.

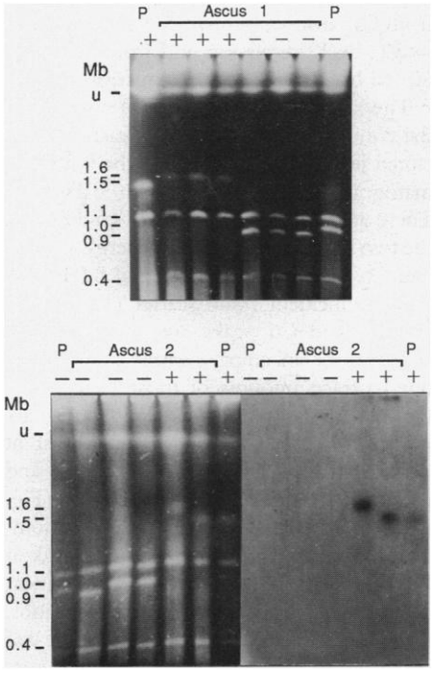

Fig. 4. Karyotypes of parents and progeny from cross 289. The parent strains are from ascus 6 of cross 272 and carry deletion derivatives of the *Pda6* chromosome. The Pda^+ parent has a 1.5-Mb derivative, whereas the Pda^- parent has a 1.0-Mb derivative. Where one progeny in an ascus showed a larger (1.6 Mb) than parental chromosome, there is a sibling from the same ascus exhibiting a correspondingly smaller (0.9 Mb) than parental band. Samples were treated as in Fig. 2.

0.9- to 1-Mb derivatives among the progeny of cross 272 and the apparent restoration of the *Pda6* chromosome to its original size in cross 289 suggest that there may be sites in the *Pda6* chromosome that are favored for breakage and reunion.

Dispensability, structural plasticity, and meiotic instability associated with karyotype change suggest that the *Pda6* chromosome of *N. haematococca* can be regarded as a B chromosome. B chromosomes have been extensively documented in plants and animals (*13*) but have only recently been reported in fungi (*14*). One major difference between the proposed B chromosome in *N. haematococca* and classical B chromosomes is the presence of at least one unique functional gene, in this case a representative from the physiologically significant *Pda* family (*1*). In addition, a *Mak* gene, which detoxifies chickpea phytoalexins, was lost concurrently with *Pda6* (7), suggesting that it is carried on the same dispensable chromosome. Unusual meiotic transmission of other *Mak* genes in *N. haematococca* has also been observed (7).

Nectria haematococca causes disease on plants other than pea and also exists as a saprophyte (*15*). In environments where pisatin is absent, the Pda^+ phenotype would not appear to be essential; thus, *Pda* genes, and apparently the chromosomes on which they reside, could be dispensable. Pisatin, however, may provide selective pressure to maintain *Pda*-containing chromosomes when the fungus is functioning as a pathogen on pea.

The frequency of meiotic loss in *N. haematococca* may be rare because the sexual cycle is infrequent in nature (*16*). Nevertheless, this study suggests that fungal genes conferring resistance to antibiotics of plant origin may be carried on nonessential components of the genome, perhaps in a manner analogous to R plasmids in bacteria. It is not yet known whether the B chromosomes are laterally transmissible, thereby conferring on different fungi one attribute for pathogenesis on pea (*17*). However, the properties of these genetic elements would suggest that they may contribute to the genetic variability of pathogenic fungi, thus altering the potential of fungi to parasitize different plants.

REFERENCES AND NOTES

1. H. D. VanEtten, D. E. Matthews, P. S. Matthews, *Annu. Rev. Phytopathol.* **27**, 143 (1989).
2. D. E. Matthews and H. D. VanEtten, *Arch. Biochem. Biophys.* **224**, 494 (1983).
3. H. D. VanEtten *et al.*, *Signal Molecules in Plants and Plant-Microbe Interactions*, vol. H36 of *North Atlantic Treaty Organization ASI Series*, B. Lugtenberg, Ed. (Springer-Verlag, Berlin, 1989), pp. 219–228.
4. H. C. Kistler and H. D. VanEtten, *J. Gen. Microbiol.* **13**, 2595 (1984).
5. S. F. Mackintosh, D. E. Matthews, H. D. VanEtten, *Mol. Plant-Microbe Interac.* **2**, 354 (1989).
6. H. D. VanEtten and P. S. Matthews, *Physiol. Plant Pathol.* **25**, 149 (1984).
7. V. P. Miao and H. D. VanEtten, *Appl. Environ. Microbiol.*, in press.

8. K. M. Weltring, B. G. Turgeon, O. C. Yoder, H. D. VanEtten, *Gene* **68**, 335 (1988).
9. V. P. Miao, D. E. Matthews, H. D. VanEtten, *Mol. Gen. Genet.* **226**, 214 (1991).
10. The presence of exclusively 4 Pda^+:4 Pda^- segregation indicates loss of *Pda6* before meiosis in this cross; however, tetrads with 6:2 segregation in other instances of *Pda6* gene loss suggest that this process might also occur during meiosis.
11. G. Chu, D. Vollrath, R. W. Davis, *Science* **234**, 1582 (1986).
12. Progeny from two or three asci collected from each of three perithecia formed by each parent of reciprocal cross 289 (a total of 13 asci) segregated 4 Pda^+:4 Pda^-. Among those examined electrophoretically, asci 2 and 5 were from the same perithecium; asci 1, 3, and 8 were each from a different perithecium.
13. R. N. Jones and H. Rees, *B Chromosomes* (Academic Press, New York, 1982).
14. D. Mills and K. McCluskey, *Mol. Plant-Microbe Interac.* **3**, 351 (1990).
15. M. C. Lucy, P. S. Matthews, H. D. VanEtten, *Physiol. Mol. Plant Pathol.* **33**, 187 (1988).
16. T. Matuo and W. C. Snyder, *Phytopathology* **62**, 731 (1972).
17. W. Schäfer, D. Straney, L. Ciuffetti, H. D. VanEtten, O. C. Yoder, *Science* **246**, 247 (1989).
18. Samples were fractionated in 0.6% agarose at 1.25 V/cm with a 52.5-min pulse time for 140 hours in 89 mM tris, 89 mM boric acid, and 2 mM EDTA at 4°C.
19. Standard techniques for Southern (DNA) analysis were used throughout. J. Sambrook, E. F. Fritsch, T. Maniatis, *Molecular Cloning* (Cold Spring Harbor Laboratory, Cold Spring Harbor, NY, 1989).
20. D. Vollrath, R. W. Davis, C. Connelly, P. Hieter, *Proc. Natl. Acad. Sci. U.S.A.* **85**, 6027 (1988).
21. M. Orbach, D. Vollrath, R. W. Davis, C. Yanofsky, *Mol. Cell. Biol.* **8**, 1469 (1988).
22. Samples were fractionated at 5.7 V/cm with a 100-s pulse time for 20 hours in 0.6% agarose.
23. H. Brody and J. Carbon, *Proc. Natl. Acad. Sci. U.S.A.* **86**, 6260 (1989).
24. The 1.6-Mb chromosome was subjected to pulsed-field electrophoresis in a 0.6% low melting point–agarose gel, then excised, and the gel slices mixed with 1 M NaCl, 25 mM tris (pH 7.5), and 1 mM EDTA. After melting at 70°C, the sample was frozen at −20°C and thawed at 37°C twice. The agarose was removed by centrifugation, and the DNA was precipitated with an equal volume of isopropanol, extracted with phenol-chloroform, and precipitated in ethanol.
25. We thank C. Wasmann and L. Ciuffetti for assistance with figure preparation. Supported in part by a Post Graduate Fellowship from the Natural Science and Research Council of Canada (to V.P.M.), by a National Science Foundation grant awarded (to S.F.C.) in 1990, and by Cooperative State Research Service–United States Department of Agriculture grant 90-37262-5292.

5 July 1991; accepted 24 October 1991

Identification and Characterization of Zinc Binding Sites in Protein Kinase C

STEVAN R. HUBBARD, W. ROBERT BISHOP, PAUL KIRSCHMEIER, SIMON J. GEORGE, STEPHEN P. CRAMER, WAYNE A. HENDRICKSON

Metal ion coordination in the regulatory domain of protein kinase C (PKC) is suggested by the conservation of six cysteines and two histidines in two homologous regions found therein. By monitoring x-ray fluorescence from a purified sample of rat PKC βI overexpressed in insect cells, direct evidence has been obtained that PKC βI tightly binds four zinc ions (Zn^{2+}) per molecule. Extended x-ray absorption fine structure (EXAFS) data are best fit by an average Zn^{2+} coordination of one nitrogen and three sulfur atoms. Of the plausible Zn^{2+} coordination models, only those featuring nonbridged Zn^{2+} sites accommodate the EXAFS data and all of the conserved potential ligands.

PKC IS A CLOSELY RELATED FAMILY of phospholipid-dependent serine/threonine kinases that play a fundamental role in cellular signal transduction (*1*). Nine different mammalian members of the PKC family have been characterized: α, βI, βII, γ, δ, ϵ, ζ [see (*1*) for a review], η (*2*), and L (*3*), and PKC homologs have been identified in *Saccharomyces cerevisiae* (*4*), *Drosophila melanogaster* (*5, 6*), and *Caenorhabditis elegans* (7).

The PKC molecule is a single polypeptide chain containing an NH_2-terminal regulatory domain and a COOH-terminal catalytic domain. The regulatory domain contains the interaction sites of the effector molecules diacylglycerol (DAG), phosphatidylserine, calcium, and tumor-promoting phorbol esters. Within the regulatory domain are two adjacent, highly similar regions of ~50 amino acids containing six conserved cysteines (C) and two conserved histidines (H) in the pattern H-X_{12}-C-X_2-C-X_{10-14}-C-X_2-C-X_4-H-X_2-C-X_7-C (C_6-H_2), where intervening X residues are more variant (Fig. 1). Exceptions to this are the ζ subtype, which contains only one C_6-H_2 region (*8*), and the L subtype, which lacks two of the conserved cysteines and one of the conserved histidines in the second C_6-H_2 region (*3*). The conservation of the six cysteines in these regions was noted early on, but the two equally conserved histidines have received little attention. This C_6-H_2 motif is also found in *n*-chimaerin (*9*), porcine diacylglycerol kinase (*10*), the *unc*-13 gene product (*11*), and the *raf/mil* (*12*) and *vav* (*13*) oncogene products. A study of PKC regulatory domain mutants has shown that the C_6-H_2 regions are essential for the binding of phorbol esters and, by implication, DAG (*14*).

Because PKC is a cytosolic protein and therefore not expected to contain disulfide bonds, a likely function served by this number of conserved cysteines is metal ion coordination. In addition, histidines are common donors of N ligands in Fe, Cu, and Zn ion coordination. The putative ligands, thiolate S and imidazole N atoms, and the absence of color of concentrated PKC solutions suggest Zn^{2+} as a candidate metal ion.

We measured the x-ray fluorescence (XRF) from a purified sample of fully activatable rat PKC βI that had been overexpressed in insect cells (*15*) (Fig. 2A). Synchrotron x-rays were used for excitation, and an energy-discriminating solid-state detector monitored XRF emissions (*16*). We could detect simultaneously a variety of metal ions, from Ca (atomic number $Z = 20$) to Ge ($Z = 32$) by K_α emission and from Sn ($Z = 50$) to Ir ($Z = 77$) by L_α emission.

The XRF data for the PKC βI sample and the control sample, a pool of fractions that eluted just before PKC βI on the last chromatography column, are shown in Fig. 2B. There are three major peaks in common in the two spectra, consistent in energy with Cr and Cu K_α emissions (5.41 and 8.04 keV) and the incident beam scatter (11.2 keV). The Cr and Cu peaks are present in the spectrum of an empty sample cell and are due to trace amounts of those elements in the cell window material. Two peaks are unique to the PKC βI spectrum, consistent with Zn K_α and K_β emissions (8.63 and 9.57 keV). In the difference spectrum (Fig. 2B inset), the Zn K_α and K_β peaks predominate. The significance of the small peak at Cu K_α is unclear. On the basis of a linear regression analysis of Zn standard solutions, the amount of Zn in the PKC βI sample was calculated to be 1.22 ± 0.03 mM. The concentration of PKC βI in the sample was determined by amino acid composition analysis and gel densitometry to be 22.2 ± 1.5 mg/ml (0.29 mM) (*17*). The calculated ratio of Zn^{2+} to PKC βI is thus 4.2 ± 0.3.

The Zn K-edge absorption spectrum for the PKC βI sample is shown in Fig. 3A, and the extracted EXAFS oscillations are shown in Fig. 3B (*18*). EXAFS can provide infor-

S. R. Hubbard and W. A. Hendrickson, Howard Hughes Medical Institute and Department of Biochemistry and Molecular Biophysics, Columbia University, New York, NY 10032.
W. R. Bishop and P. Kirschmeier, Schering-Plough Research, Bloomfield, NJ 07003.
S. J. George, Department of Applied Sciences, University of California, Davis, CA 95616.
S. P. Cramer, Department of Applied Sciences, University of California, Davis, CA 95616, and Division of Applied Science, Lawrence Berkeley Laboratory, Berkeley, CA 94720.